3D QSAR studies based in silico screening of 4,5,6-triphenyl-1,2,3,4-tetrahydropyrimidine analogs for anti-inflammatory activity

ARTICLE *in* EUROPEAN JOURNAL OF MEDICINAL CHEMISTRY · DECEMBER 2013

Impact Factor: 3.45 · DOI: 10.1016/j.ejmech.2013.10.083 · Source: PubMed

3 AUTHORS:

Deepak Lokwani
Dr. Babasaheb Ambedkar Marathwada Uni…
19 PUBLICATIONS **100** CITATIONS
SEE PROFILE

Santosh N Mokale
Y. B. Chavan College of Pharmacy
24 PUBLICATIONS **71** CITATIONS
SEE PROFILE

Devanand Shinde
Dr. Babasaheb Ambedkar Marathwada Uni…
279 PUBLICATIONS **1,606** CITATIONS
SEE PROFILE

European Journal of Medicinal Chemistry 73 (2014) 233–242

Contents lists available at ScienceDirect

European Journal of Medicinal Chemistry

journal homepage: http://www.elsevier.com/locate/ejmech

Original article

3D QSAR studies based *in silico* screening of 4,5,6-triphenyl-1,2,3,4-tetrahydropyrimidine analogs for anti-inflammatory activity

Deepak K. Lokwani [a], Santosh N. Mokale [b], Devanand B. Shinde [a,*]

[a] Department of Chemical Technology, Dr. Babasaheb Ambedkar Marathwada University, Aurangabad 431004, M.S., India
[b] Dr. Rafiq Zakaria Campus, Y.B. Chavan College of Pharmacy, Aurangabad 431001, M.S., India

ARTICLE INFO

Article history:
Received 9 April 2013
Received in revised form
16 October 2013
Accepted 21 October 2013
Available online 25 December 2013

Keywords:
3D QSAR
Anti-inflammatory
COX-2
1,2,3,4-Tetrahydropyrimidine
Common Pharmacophore Hypotheses (CPHs)

ABSTRACT

The 3D QSAR studies based on generation of common pharmacophore hypotheses (CPHs) were performed separately for the series of 1,2,3,4-tetrahydropyrimidin-5-yl-acetic acid and 2-(4-sulfonylphenyl) pyrimidine analogs for their *in-vivo* anti-inflammatory activity and *in-vitro* COX-2 inhibitory activity respectively. The main idea of selecting two different series was to develop two 3D QSAR models for same scaffold (1,2,3,4-tetrahydropyrimidine/pyrimidine) for same target, but with different aspects of activity. The aim of study was to screen designed compounds and select new compounds with increased COX-2 selectivity. The best 3D QSAR model from both group was employed as 3D search query to screen the designed 4,5,6-triphenyl-1,2,3,4-tetrahydropyrimidine derivatives. The new compounds showing good predicted activity were selected for experimental studies. Among the synthesized compounds, **5c** and **5f** showed highest anti-inflammatory activity.

1. Introduction

The discovery of two distinct isoforms (COX-1 and COX-2) of enzyme Cyclooxygenase (COX) in 1990s led to the development of a new class of Nonsteroidal anti-inflammatory drugs (NSAIDs), selective for COX-2, named coxibs [1]. COX-2 is primarily responsible for proinflammatory conditions, while COX-1 is constitutive and responsible for the maintenance of physiological homeostasis, such as gastrointestinal integrity and renal function [2]. Thus the selective COX-2 inhibitors provided a potential class of anti-inflammatory agents which overcomes the gastrointestinal (GI) side effects associated with use of traditional NSAIDs (t-NSAIDs). However, the long-term use of both t-NSAIDs and coxibs has been reported to cause significant cardiovascular effects, myocardial infarctions, and strokes. Unfortunately, the withdrawal of rofecoxib from market in the fall of year 2004 after its clinical report of its linkage to increased risk of cardiovascular toxicity has widely affected the safety of coxib [3,4]. But it is still remains dubious whether the observed cardiovascular toxicity of rofecoxib is a class effect or individually drug specific. Hence, the conflict associated with coxib can only be reduced by development of new generation of COX-2 inhibitors to avoid the unwanted cardiac effects.

The search for COX selective inhibitors is somewhat complicated by the close structural similarities between COX-1 and COX-2. Both COX-1 and COX-2 are homodimers of 70 kDa subunits composed of N-terminal epidermal growth factor like module, α-helical membrane binding domain and a large C-terminal globular catalytic domain with active site (Cyclooxygenase and peroxidase containing heme cofactor) [5]. COX catalytic domain in COX-2 is 20% larger and differs in the presence of side pocket when compared to COX-1. The main and important difference in side pocket is the presence of valine in COX-2 and isoleucine in COX-1 at position 523 which enables interaction of the sulfonamide or sulfone group of the coxibs with Arg 513 in the side pocket of COX-2 [6]. The X-ray crystallography, kinetic studies, and molecular modeling are among the most explored tools to understand both the selectivity and binding mode of nonselective and selective inhibitors. Therefore, these approaches constitute the primary source of information toward the rational drug design of novel selective COX-2 inhibitors.

The major class of coxibs possess 1,2-diarylsubstitution on a central hetero or carbocyclic ring system with a characteristic methanesulfonyl, sulfonamido, or methanesulfonamide group on one of the aryl rings that plays a crucial role for COX-2 selectivity [7–9]. Recently, we have reported a series of 1,2,3,4-tetra

* Corresponding author. Tel.: +91 240 2403308.
E-mail address: dbsdeepak10@rediffmail.com (D.B. Shinde).

0223-5234/$ – see front matter © 2013 Elsevier Masson SAS. All rights reserved.
http://dx.doi.org/10.1016/j.ejmech.2013.10.083

hydropyrimidine analogs containing triaryl ring rather than diaryl with good selectivity for COX-2 over COX-1 isoform [10].

In this study, we have reported synthesis and biological evaluation of new 4,5,6-triaryl-1,2,3,4-tetrahydropyrimidine analogs as COX-2 inhibitors. On which aryl ring, *p*-methylsulfonyl or *p*-aminosulfonyl is being to be substituted, based on this concept, new analogs were designed. For the screening of designed compounds, two 3D QSAR models were developed based on generation of Common pharmacophore hypotheses (CPHs). The 3D QSAR model I was developed for 1,2,3,4-tetrahydropyrimidin-5-yl-acetic acid reported for *in-vivo* anti-inflammatory activity and the 3D QSAR model II was developed for 2-(4-sulfonylphenyl)pyrimidines analogs for their *in-vitro* COX-2 inhibitory activity (Fig. 1). The aim of selecting two different series with *in-vivo* and *in-vitro* anti-inflammatory activity for 3D QSAR studies was to find new compounds with high affinity for COX-2 enzyme. The generated models were used as search query to virtually screen designed 4,5,6-triaryl-1,2,3,4-tetrahydropyrimidine analogs. The ten new compounds were selected, synthesized and evaluated for anti-inflammatory activity.

2. Result and discussion

2.1. Development of QSAR model I and 3D QSAR model II

The thirty six 1,2,3,4-tetrahydropyrimidin-5-yl-acetic acid derivatives with their *in-vivo* anti-inflammatory activity [11,12] were selected for 3D QSAR model I, based on the criteria that the designed 4,5,6-triaryl-1,2,3,4-tetrahydropyrimidine derivatives are the optimized analogs of this selected series. The 3D QSAR models developed for this series will be helpful to predict correctly the activity of new untested compounds. The twenty three 2-(4-sulfonylphenyl)pyrimidine derivatives reported as COX-2 inhibitors [13] were selected for development of 3D QSAR model II with aim to predict the COX-2 inhibiting activity of the new untested compounds. For the sake of study to develop 3D QSAR model

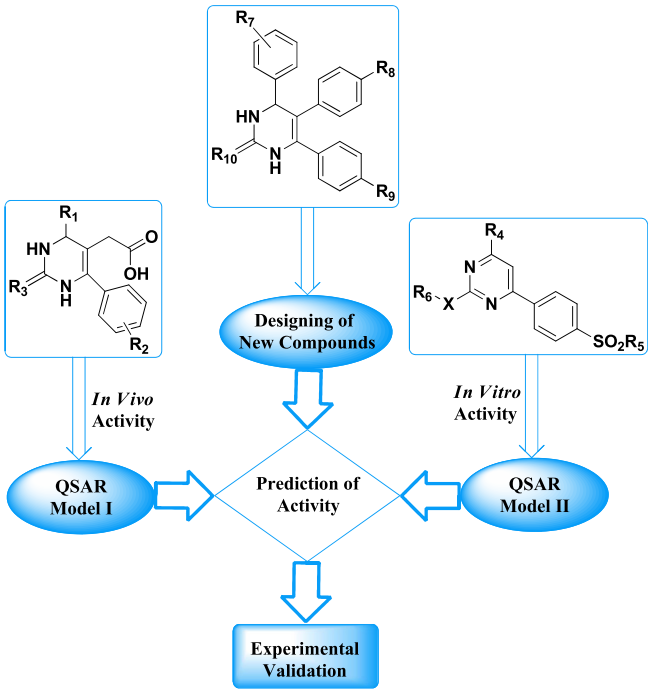

Fig. 1. Flow chart of *in silico* screening using 3D QSAR studies.

I, percent inhibition of inflammation (i.e., reduction in rat paw edema volume) by 1,2,3,4-tetrahydropyrimidin-5-yl-acetic acid derivatives was transformed [14,15] into the log activity using Equation (1). Whereas pIC_{50} (log $(1/IC_{50})$) values of 2-(4-sulfonylphenyl)pyrimidines derivatives against COX-2 inhibition were used for generation of 3D QSAR model II.

$$\text{Log Activity} = -\log c + \log it \quad (1)$$

Where,

'c' (molar concentration) = concentration (μg/ml) × 0.001/molecular weight,
'it' stands for inhibition and log it = log [% inhibition/100 − % inhibition]

The variant CPHs were generated, examined and scored to identify the common pharmacophore that yields the best alignment of the active compounds (log activity > 0.817 for QSAR model I and pIC_{50} > 2.80 for QSAR model II). All CPHs were validated by aligning and scoring the inactive compounds (log activity < 0.510 for QSAR model I and pIC_{50} < 1.60 for QSAR model II). The CPH's models whose the survival-inactive scores ranked in the top 1% for alignment of all compounds were selected for development of both 3D-QSAR model I and 3D-QSAR model II. The CPHs selected for development of 3D QSAR model I and 3D-QSAR model II were found to have the three-point features (one negatively charged group (N) and two aromatic Rings (R) features) and the five-point features (four hydrogen bond acceptor (A), and one aromatic ring (R) features) respectively. The 3D QSAR model I and 3D QSAR model II were constructed with twenty six and eighteen compounds included in training set with diverse activity respectively (Tables 1 and 2). The rest of compounds in both series were kept aside as a test set for validation and testing of constructed 3D QSAR models. The 3D QSAR models were generated using Partial Least Square (PLS) regression method. One model in each category of 3D QSAR model I and 3D QSAR model II was selected based on statistical results and comparison of experimental and predicted activity (log activity for 3D QSAR model I and pIc_{50} for QSAR model II). The R^2, SD, F, P and stability results were used to evaluate the training set predictions and the Q^2, RMSE and Pearson-R values were used to evaluate the test set prediction (Table 3).

2.2. Analysis of 3D QSAR models

The contribution map obtained from 3D QSAR models identifies features of ligands for interaction with target protein. Thus map identifies particular position in ligand that requires specific physicochemical properties to enhance the bioactivity of ligands. A pictorial representation of the contribution map is shown in Fig. 2a–d and 3a–f. In these representations, blue cubes indicate favorable features and red cubes represent unfavorable features in compounds for activity. The equal positive and negative thresholds were set while visualizing the 3D QSAR in context of all ligands.

2.2.1. 3D QSAR model I

Fig. 2a–d shows the visualization of results of 3D QSAR model I when applied to compounds in the series of 1,2,3,4-tetrahydropyrimidin-5-yl-acetic acid derivatives (Table 1). As per the common pharmacophore of 1,2,3,4-tetrahydropyrimidin-5-yl-acetic acid derivatives, the changes in nature of substituents are seen in combined hydrophobic and electronegative features at $\mathbf{R_1}$ position and hydrophobic features at $\mathbf{R_2}$ position. When these above hydrophobic and electronegative features visualized individually or combined in context of most active compound **A27** and

Table 1
1,2,3,4-Tetrahydropyrimidin-5-yl-acetic acid derivatives selected for generation of 3D QSAR model I and their observed and predicted activity.

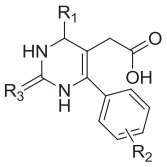

A1-A18: **R_3= -NH**; A19-A36: **R_3 = -S**

Sr. no.	R_1	R_2	Observed activity (log activity)	Predicted activity	Residual
A1	$-C_6H_5$	H	0.64	0.7	−0.06
A2[a]	$-C_6H_4$-4-Cl	H	0.64	0.51	0.13
A3[a]	$-C_6H_4$-4-OCH_3	H	0.82	0.9	−0.08
A4	−2-Thiophene	H	0.51	0.59	−0.08
A5[a]	−2-Furan	H	0.55	0.45	0.1
A6	−3-Pyridine	H	0.30	0.32	−0.02
A7	$-C_6H_5$	Cl	0.78	0.73	0.05
A8[a]	$-C_6H_4$-4-Cl	Cl	0.74	0.78	−0.04
A9	$-C_6H_4$-4-OCH_3	Cl	0.92	0.89	0.03
A10	−2-Thiophene	Cl	0.64	0.63	0.01
A11	−2-Furan	Cl	0.56	0.58	−0.02
A12	−3-Pyridine	Cl	0.54	0.51	0.03
A13	$-C_6H_5$	CH_3	0.82	0.81	0.01
A14	$-C_6H_4$-4-Cl	CH_3	0.68	0.78	−0.1
A15	$-C_6H_4$-4-OCH_3	CH_3	0.88	0.93	−0.05
A16	−2-Thiophene	CH_3	0.64	0.63	0.01
A17	−2-Furan	CH_3	0.54	0.53	0.01
A18	−3-Pyridine	CH_3	0.58	0.5	0.08
A19[a]	$-C_6H_5$	H	0.52	0.7	−0.18
A20	$-C_6H_4$-4-Cl	H	0.88	0.77	0.11
A21[a]	$-C_6H_4$-4-OCH_3	H	0.92	0.85	0.07
A22[a]	−2-Thiophene	H	0.64	0.51	0.13
A23	−2-Furan	H	0.57	0.55	0.02
A24	−3-Pyridine	H	0.46	0.34	0.12
A25	$-C_6H_5$	Cl	0.65	0.72	−0.07
A26	$-C_6H_4$-4-Cl	Cl	0.82	0.79	0.03
A27	$-C_6H_4$-4-OCH_3	Cl	1.02	1.00	0.02
A28	−2-Thiophene	Cl	0.54	0.56	−0.02
A29[a]	−2-Furan	Cl	0.24	0.47	−0.23
A30	−3-Pyridine	Cl	0.35	0.26	0.09
A31	$-C_6H_5$	CH_3	0.82	0.72	0.1
A32	$-C_6H_4$-4-Cl	CH_3	0.72	0.79	−0.07
A33[a]	$-C_6H_4$-4-OCH_3	CH_3	0.96	0.86	0.1
A34	−2-Thiophene	CH_3	0.28	0.29	−0.01
A35[a]	−2-Furan	CH_3	0.31	0.47	−0.16
A36	−3-Pyridine	CH_3	0.11	0.34	−0.23

[a] Compounds in test set.

least active compound **A36**, the blue cubes were observed around methoxy group of phenyl ring at **R_1** position and chloro group at **R_2** position in compound **A27**. Whereas red cubes were seen around pyridine ring at **R_1** position in compound A36 (Fig. 2a and b). This suggested that the phenyl ring (hydrophobic features) with electron donating groups at **R_1** position is important for activity. The less hydrophobic features or changing in the position of electronegative groups decreases the activity of compounds. Thus the compound **A36** show red cubes around pyridine ring. Similarly other compounds **A4**, **A5**, **A6** and many more in the series containing hetero ring at **R_1** position shows the red cubes (Fig. 2c) and thus the less active as compared to the compounds containing phenyl ring or substituted phenyl ring at **R_1** position. While comparing the substitution pattern at **R_2** position, some blue cubes are found around chloro and methyl group in compounds **A27**, **A11**, **A15**, **A34** and many more in series. But replacement of these groups by hydrogen in compounds **A3**, **A5** and many more in series, not

Table 2
2-(4-Sulfonylphenyl)pyrimidine derivatives selected for generation of 3D QSAR model II and their observed and predicted activity.

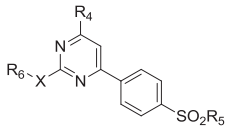

B1-B17, B19-B23: **R_4 = -CF_3**; B18: **R_4 = -OCH_2CF_3**

Sr. no.	R_5	X	R_6	Observed activity (PIC_{50})	Predicted activity	Residual
B1	$-CH_3$	−NH−	$-C_6H_5$	2.25	2.30	−0.05
B2	$-CH_3$	−NH−	$-C_6H_4$, -4-CH_3	1.95	2.30	−0.35
B3[a]	$-CH_3$	−NH−	$-C_6H_4$-4-F	2.14	2.30	−0.16
B4	$-CH_3$	−NH−	$-CH_2C_6H_5$	3.6	3.40	0.20
B5	$-CH_3$	−NH−	$-CH_2C_6H_4$-4-CH_3	2	1.64	0.36
B6	$-CH_3$	−NH−	$-CH_2C_6H_4$-4-F	3.55	3.67	−0.12
B7	$-CH_3$	−NH−	−H	0.56	0.57	0.00
B8	$-CH_3$	−NH−	$-CH_2CH_3CH_3$	2.3	2.30	0.00
B9	$-CH_3$	−NH−	$-n$-$CH_2CH_3CH_3CH_3$	2.88	2.89	−0.01
B10[a]	$-NH_2$	−NH−	$-n$-$CH_2CH_3CH_3CH_3$	2.85	2.85	0.00
B11	$-CH_3$	−NH−	$-i$-$CH_2CH_3CH_3CH_3$	2.69	2.70	−0.01
B12	$-CH_3$	−NH−	$-C_6H_{11}$	3.3	3.30	0.00
B13[a]	$-NH_2$	−NH−	$-C_6H_{11}$	2.61	2.42	0.19
B14	$-CH_3$	−NH−	$-CH_2C_6H_{11}$	1.53	1.54	−0.01
B15	$-CH_3$	−NH−	−4-Tetrahydro-2*H*-pyran	1.74	1.75	−0.01
B16	$-CH_3$	−NH−	−4-Methyltetrahydro-2*H*-pyran	2.3	2.30	0.00
B17	$-CH_3$	$-NCH_3-$	$-CH_2C_6H_5$	2.3	2.52	−0.22
B18	$-CH_3$	−NH−	$-C_6H_{11}$	1.79	1.80	−0.01
B19[a]	$-CH_3$	−O−	$-n$-$CH_2CH_3CH_3CH_3$	1.66	1.67	−0.01
B20	$-CH_3$	−O−	$-i$-$CH_2CH_3CH_3$	1.2	1.20	0.00
B21	$-CH_3$	−O−	$-t$-$CH_2CH_3CH_3CH_3$	1.48	1.48	0.00
B22	$-CH_3$	−O−	$-CH_2C_5H_9$	1.65	1.66	−0.01
B23[a]	$-CH_3$	−O−	$-CH_2C_6H_{11}$	1.34	1.35	−0.01

[a] Compounds in test set.

show any blue cubes (Fig. 2a–d). This suggests the presence of hydrophobic features at **R_2** position is important for activity.

2.2.2. 3D QSAR model II

Fig. 3a–f shows the visualization of results of 3D QSAR model II when applied to compounds in the series of 2-(4-sulfonylphenyl) pyrimidines derivatives (Table 2). For the simplicity and for comparing the inhibitory activity of compounds, H-bond donor and hydrophobic features were selected and visualized in the context of active, moderate and inactive compounds in the series. When visualizing the H-bond donor features in context of compounds, the blue cubes were seen around −NH group at **X** position in compounds **B1**–**B16** and no blue or red cubes were seen around $-NCH_3$ and −O group at **X** position in compounds **B17 and B19**–**B23** respectively (Fig. 3a–c). This suggests that H-bond donor features at **X** position are important for activity. Similarly when visualizing the hydrophobic features in the context of compounds, the blue

Table 3
Statistical results for QSAR model I and QSAR model II.

Sr. no.	Statistical parameters	QSAR model I	QSAR model II
1	SD	0.0841	0.2613
2	R^2	0.8733	0.8139
3	*F*	36.2	19
4	*P*	$3.87E^{-09}$	$4.987e^{-05}$
5	Stability	0.5073	0.3688
6	RMSE	0.1346	0.1203
7	Q^2	0.6512	0.955
8	Pearson-R	0.8114	0.9793

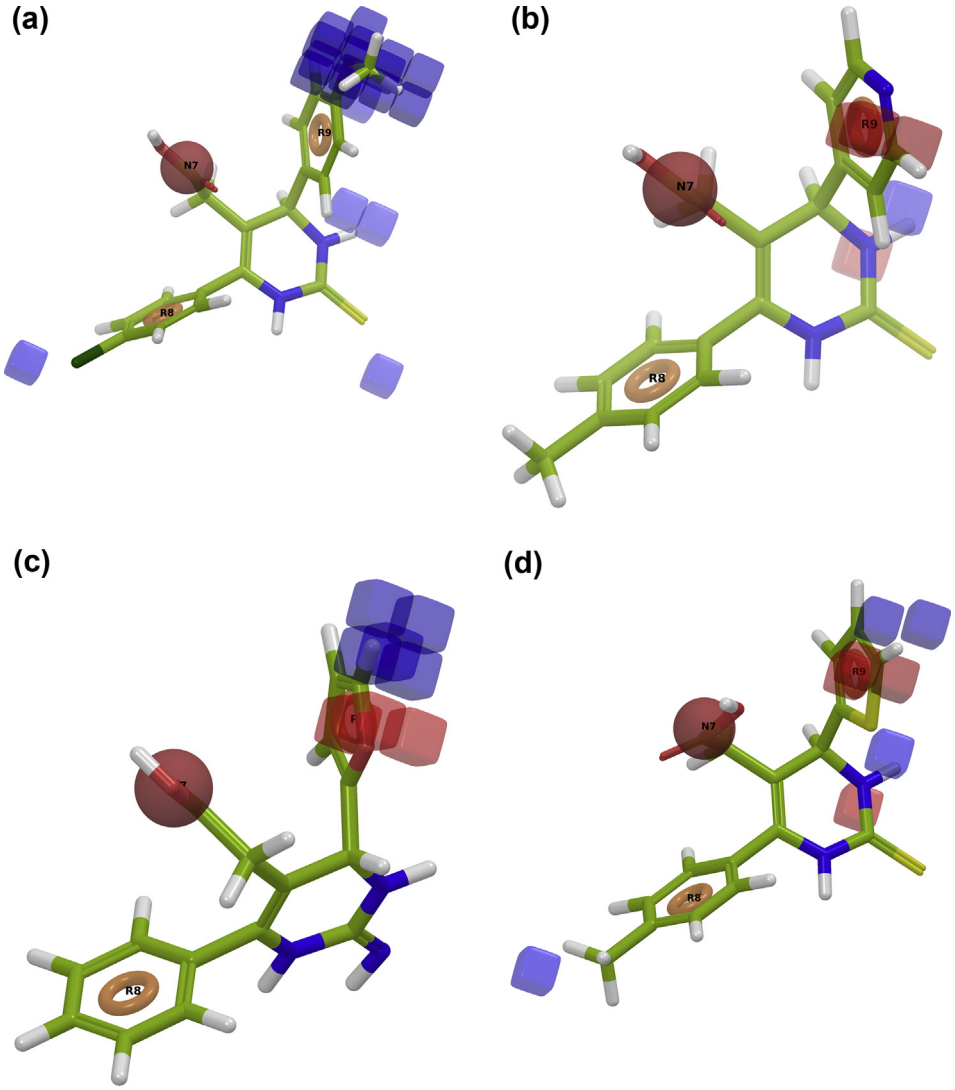

Fig. 2. Pictorial representation of the cubes generated using the 3D QSAR model I. Blue cubes indicate favorable regions, while red cubes indicate unfavorable region for the activity. QSAR model visualized in the context of favorable and unfavorable feature for (a) compound **A27**, (b) compound **A36**, (c) compound **A5** and (d) compound **A34**. (For interpretation of the references to color in this figure legend, the reader is referred to the web version of this article.)

cubes were found around phenyl ring or substituted phenyl ring at $\mathbf{R_6}$ position in compounds **B1**–**B6** and many more in series (Fig. 3d). Whereas the mixed blue and red cubes were found when $\mathbf{R_6}$ position is unsubstituted as in compound B7 (Fig. 3e) or substituted by aliphatic chain or hetero ring as in compounds **B8**–**B11**, **B15**, **B16** and **B19**–**B21** (Fig. 3f). This indicated that presence of phenyl ring or substituted phenyl ring at $\mathbf{R_6}$ position is important for activity. The small hydrophobic features at $\mathbf{R_4}$ position are also important for activity, as the presence of $-CF_3$ group shows blue cubes around it in compounds, whereas the replacement of this group by $-OCH_2CF_3$, shows the red cubes around it.

2.3. Screening of designed compounds and their synthesis

All designed compounds were first screened by predicting their ADMET properties using Qikprop v3.5 (Schrödinger, LLC, New York, NY, 2012). The compounds following Lipinski's rule and other ADMET properties were selected further for the prediction of their activity using QSAR Model I and QSAR model II. The ten designed compounds were selected for experimental validation (Table 4). These compounds were selected based on criteria that compounds showed good predicted activity against either both QSAR models or individual QSAR model.

The synthetic route of selected designed 4,5,6-triphenyl-1,2,3,4-tetrahydropyrimidine derivatives is outlined in Schemes 1 and 2. The compounds **5a**–**g** were synthesized in major four steps. The starting material, 1-(4-(methylthio)phenyl)-2-phenylethanone (**3a**) was synthesized in two steps using intermediate phenyl acetyl chloride (**2**) which was prepared by chlorination of phenyl acetic acid (**1**) using thionyl chloride. The synthesized phenyl acetyl chloride was then made to react with thioanisole in dichloromethane in the presence of anhydrous $AlCl_3$ to undergo Friedel–Crafts acylation which gave 1-(4-(methylthio)phenyl)-2-phenylethanone (**3a**) [10]. The methylthio group in compound **3a** was then oxidized by oxane in presence of acetone-water to methylsulfonyl group which gave 1-(4-(methylsulfonyl)phenyl)-2-phenylethanone (**4a**) [16]. The final compounds **5a**–**g** were then synthesized using one pot Biginelli reaction of **4a**, substituted aldehyde and urea/thiourea/guanidine hydrochloride in the presence of potassium carbonate and ethanol as solvent [10–12].

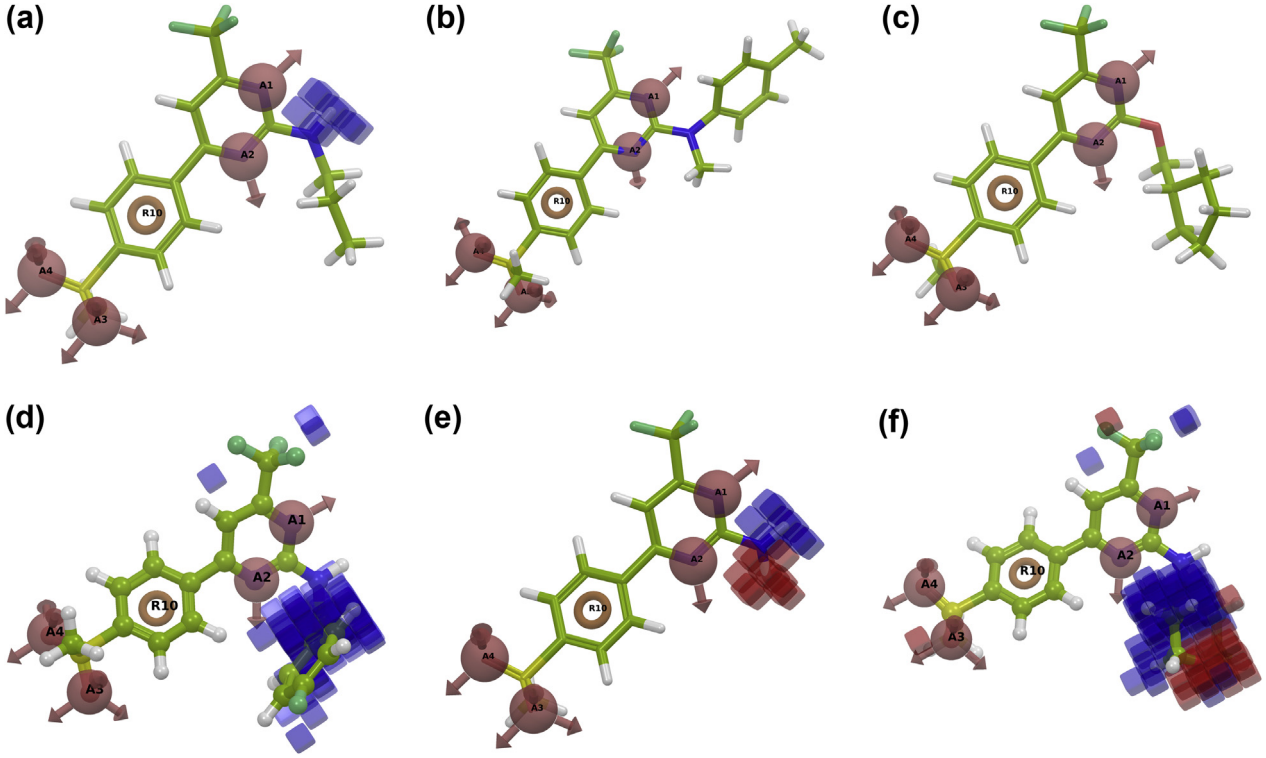

Fig. 3. Pictorial representation of the cubes generated using the 3D QSAR model II. Blue cubes indicate favorable regions, while red cubes indicate unfavorable region for the activity. QSAR model visualized in the context of favorable and unfavorable H-bond donor features for (a) compound **B8**, (b) compound **B17** and (c) compound **B22**. QSAR model visualized in the context of favorable and unfavorable hydrophobic features for (d) compound **B6**, (e) compound **B7** and (f) compound **B15**. (For interpretation of the references to color in this figure legend, the reader is referred to the web version of this article.)

1-(4-Chlorophenyl)-2-phenylethanone (**3b**) was prepared as described for the synthesis of compounds **3a** and was further used for synthesis of final compounds **5h**–**j**. The treatment of compound **3b** with chlorosulfonic acid yielded their corresponding sulfonyl chloride derivative (**4b**) which was subsequently triturated with ammonium carbonate to yield the sulfonamide derivative (**4e**). The methyl sulfonamide derivative (**4d**) was obtained by methylation of the sodium salt of compound **4b** with methyl iodide in tetrahydrofuron as demonstrated in Scheme 2. The final compounds **5h**–**j** were then synthesized from compounds **4d** and **4e** by reaction with substituted aldehyde and urea/guanidine hydrochloride in the presence of potassium carbonate and ethanol as solvent.

2.4. Biological screening

Anti-inflammatory activity of the all synthesized compounds was evaluated by carrageenan-induced rat paw edema model (Table 5). The onset of action was evident during 1 h in various test groups. All the tested compounds showed reasonable percentages of reduction of edema up to 4 h. Among the tested compounds, **5c** and **5f** showed highest percent inhibition of edema up to 4 h which was comparable to percent inhibition of edema induced by celecoxib. It was observed from *in vivo* results that the presence of $-SO_2CH_3$ at $\mathbf{R_9}$ position is important for anti-inflammatory activity whereas compounds with $-SO_2CH_3$ at $\mathbf{R_8}$ position showed reduced anti-inflammatory activity. The presence of electron donating group ($-N(CH_3)_2$) at $\mathbf{R_7}$ position in compound **5c** proves the prediction of 3D QSAR model I that presence of combined phenyl ring (hydrophobic features) with electron donating groups at $\mathbf{R_1}$ position of 1,2,3,4-tetrahydropyrimidin-5-yl-acetic acid derivatives showed increased anti-inflammatory activity (Table 1). Thus in synthesized series, the compound **5c** was found to be more potent anti-inflammatory compound. The reduction of electron donating features at $\mathbf{R_7}$ position in 4,5,6-triphenyl-1,2,3,4-tetrahydropyrimidine derivatives decrease the anti-inflammatory activity. However we found compound **5f** with unsubstituted phenyl ring at $\mathbf{R_7}$ position showed similar anti-inflammatory activity as that of compound **5c**. Compound **5h** with OCH_3 group at $\mathbf{R_7}$ position and $-SO_2CH_3$ group at $\mathbf{R_8}$ position was also found to show increased anti-inflammatory activity after 3 h which continued up to 24 h. The compounds **5c** and **5f** were further tested for COX-2 selectivity and it was found from *in vitro* COX-2 assay that both compounds showed good COX-2 inhibiting activity at 20 μM concentration with minimal inhibition of COX-1 enzyme (Table 6).

3. Conclusion

The development of two 3D QSAR models, QSAR model I for 1,2,3,4-tetrahydropyrimidin-5-yl-acetic acid for *in-vivo* anti-inflammatory activity and QSAR model II for 2-(4-sulfonylphenyl) pyrimidines analogs for *in-vitro* COX-2 inhibitory activity has been described with aim to screen designed 4,5,6-triphenyl-1,2,3,4-tetrahydropyrimidine derivatives. The ten new compounds were selected on the basis of activity predicted by both models, synthesized and screened for their anti-inflammatory activity. The compounds **5c** and **5f** were found to be potent with highest *in vivo* anti-inflammatory activity. It was also found that presence of electron donating moiety at $\mathbf{R_7}$ and SO_2CH_3 group at $\mathbf{R_9}$ position of 4,5,6-triphenyl-1,2,3,4-tetrahydropyrimidine derivatives is necessary for anti-inflammatory activity. The compounds **5c** and **5f** further showed comparable COX-2 inhibition with that of celecoxib. The overall results of experimental studies thus suggested that ligand based 3D QSAR study could be useful method for lead optimization. The pharmacophoric features obtained from both 3D

Table 4
Structures of selected designed compounds for experimental studies along with their predicted activity.

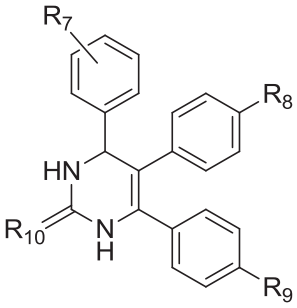

Comp.	R_7	R_8	R_9	R_{10}	Predicted activity	
					QSAR model I	QSAR model 2
5a	$-3,4\text{-}OCH_3$	$-H$	$-SO_2CH_3$	$-NH$	0.74	NP[a]
5b	$-2,5\text{-}OCH_3$	$-H$	$-SO_2CH_3$	$-NH$	0.52	1.8
5c	$-4\text{-}N(CH_3)_2$	$-H$	$-SO_2CH_3$	$-O$	0.78	1.6
5d	$-2,5\text{-}OCH_3$	$-H$	$-SO_2CH_3$	$-O$	0.47	1.82
5e	$-2,4\text{-}OCH_3$	$-H$	$-SO_2CH_3$	$-O$	0.52	1.82
5f	H	$-H$	$-SO_2CH_3$	$-S$	0.52	1.4
5g	$-2,4\text{-}OCH_3$	$-H$	$-SO_2CH_3$	$-S$	0.54	1.51
5h	$-4\text{-}OCH_3$	$-SO_2CH_3$	$-Cl$	$-NH$	0.73	NP
5i	$-4\text{-}N(CH_3)_2$	$-SO_2CH_3$	$-Cl$	$-O$	0.71	NP
5j	$-2,5\text{-}OCH_3$	$-SO_2NH_2$	$-Cl$	$-O$	0.5	1.69

[a] NP – not predicted.

QSAR models and structure activity relationship of experimental studies will be useful further to optimize 1,2,3,4-tetrahydropy rimidine scaffold.

4. Experimental studies

4.1. Generation of 3D QSAR model

Phase v3.3 (Schrödinger, LLC, New York, NY, 2012) implemented in Maestro v9.2 (Schrödinger, LLC, New York, NY, 2012) was used for the pharmacophore generation and 3D QSAR studies [6]. Biological data used for 3D QSAR studies was divided into a training set and a test set in such a way that they contained information in terms of both their structural features and biological activity ranges. The most active molecules, moderately active, and less active molecules were included in training set to spread out the range of activities whereas the test compounds were selected in such a way that they truly represent the training set. The structure of each compounds were cleaned and optimized using Ligprep v2.4 (Schrödinger, LLC, New York, NY, 2012).

Phase provide a built-in set of six pharmacophore features such as hydrogen bond acceptor (A), hydrogen bond donor (D), hydrophobic group (H), negatively charged group (N), positively charged group (P), and aromatic ring (R), defined by a set of chemical structure patterns as SMARTS queries. Common pharmacophoric features were then identified from a set of variants (set of feature types) that define a possible pharmacophore using a tree based partitioning algorithm with maximum tree depth of four with the requirement that all actives must match. After applying default feature definitions to each ligand, CPHs were generated using a final box of 1 Å. All generated CPHs were examined and selected based on a scoring function to yield the best alignment of the active ligands using an overall maximum Root Mean Square Deviation (RMSD) value of 1.2 Å with default options for distance tolerance. The quality of alignment was measured by a survival score.

Atom-based 3D QSAR models were developed using Partial Least Squares (PLS) regression analysis. In atom-based 3D QSAR in Phase, each molecule was treated as a set of overlapping Vander Waals spheres. Each atom (and hence each sphere) was placed into one of six categories according to a simple set of rules: hydrogens attached to polar atoms were classified as hydrogen bond donors (D); carbons, halogens, and C–H hydrogens are classified as hydrophobic/non-polar (H); atoms with an explicit negative ionic charge are classified as negative ionic (N); atoms with an explicit positive ionic charge were classified as positive ionic (P); non-ionic atoms were classified as electron-withdrawing (W); and all other types of atoms were classified as miscellaneous (X). For Construction of atom-based 3D QSAR model, a rectangular grid of cubes (1 Å on each side) were defined for aligned training set for occupation of all atoms. Each occupied cubes were allotted one or more volume bits to represent the molecules by string of zero and ones. This representation gives rise to binary-valued occupation patterns that

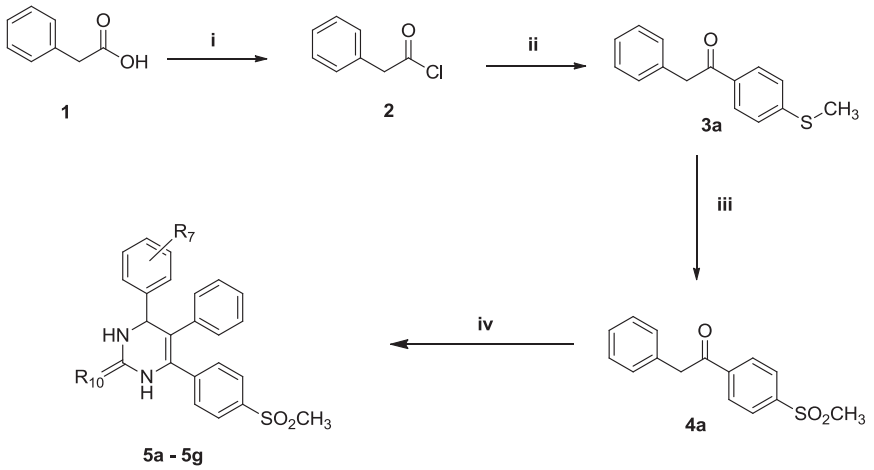

(i) $SOCl_2$ (ii) thioanisole in CH_2Cl_2, $AlCl_3$ (iii) Oxane, Acetone-Water (iv) aromatic aldehydes, urea/thiourea/guanidine HCl in ethanol, K_2CO_3

Scheme 1. Synthesis of compounds **5a–g**.

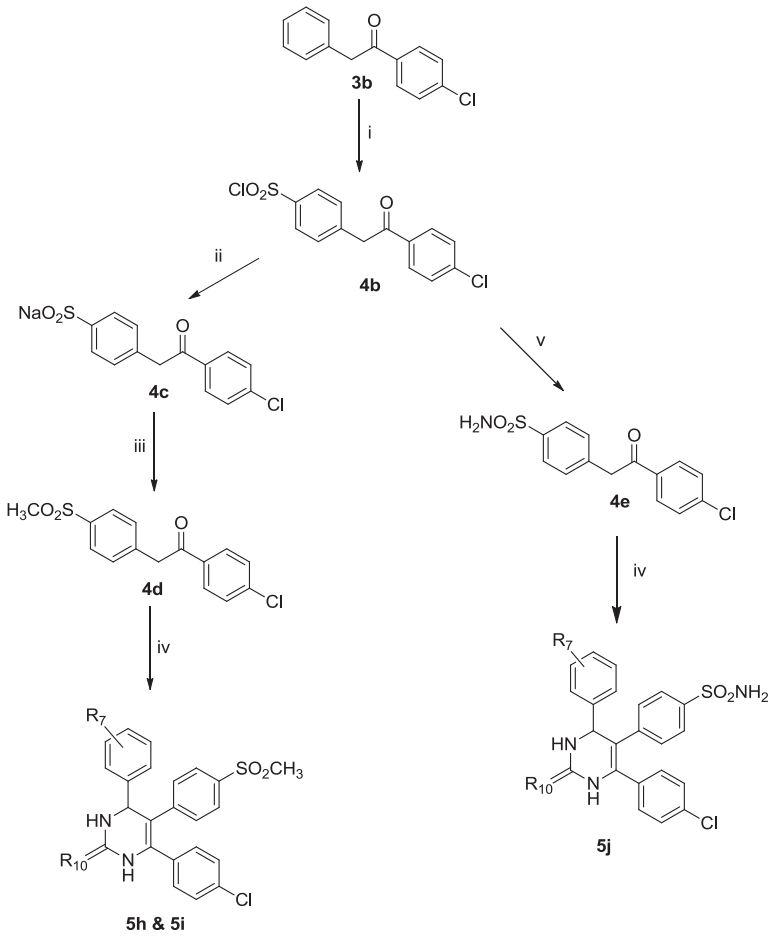

(i) Chlorosulfonic acid (ii) Na_2SO_3, $NaHCO_3$ (iii) $NaHCO_3$, dimethyl sulfate (iv) aromatic aldehydes, urea/guanidine HCl in ethanol, K_2CO_3 (v) NH_4OH, reflux then Conc. HCl

Scheme 2. Synthesis of Compounds **5h**–**j**.

was used as independent variables to create PLS QSAR models. The PLS regression was carried out with maximum of N/5 PLS factors, N = number of ligands in training set.

4.2. Synthesis

The purities of all the synthesized compounds have been checked by thin-layer chromatography (TLC) using various non-aqueous solvents. Melting points were determined on SRS OPTI-MELT and were uncorrected. ^{1}H NMR spectra and ^{13}C NMR were recorded on a Bruker DXM-400 spectrometer (400 MHz) with $CDCl_3$ as a solvent. Mass spectra were recorded on time of flight mass spectrometer.

4.2.1. Synthesis of 1-(4-(methylsulfonyl)phenyl)-2-phenylethanone (*4a*)

To a suspension of 1-(4-(methylthio)phenyl)-2-phenylethanone (**3a**) (2.43 mmol) in acetone-water (2:1), Oxone (4.03 mmol) was added and the mixture was stirred at RT for 2 h. After completion of the reaction, acetone was removed under low vacuum and the resulting mixture was diluted with cold water (25 ml). The mixture was then extracted with ethyl acetate (3 × 25 ml). The organic layer was collected, combined and washed with cold water (2 × 25 ml), dried over anhydrous sodium sulfate, filtered and concentrated to give the title compound.

Yield (solid): 70.8%; M.P.: 161.3–163.1 °C; FT-IR (neat) cm^{-1}: 3008, 2962, 1680, 1270; ^{1}H NMR (400 MHz, $CDCl_3$): $\delta = 3.23$ (s, 3H), 4.26 (s, 2H), 7.20–7.32 (m, 6H), 7.97–8.03 (m, 3H); ^{13}C NMR (400 MHz, $CDCl_3$): $\delta = 40.80$, 44.12, 117.43, 123.76, 127.28, 130.30, 132.45, 190.10; AP-MS: $m/z = 275.3$ $[M + H]^+$.

4.2.2. Synthesis of 1-(4-chlorophenyl)-2-(4-(methylsulfonyl) phenyl)ethanone (*4d*)

1-(4-Chlorophenyl)-2-phenylethanone (**3b**) (0.05 mol) was added slowly to chlorosulfonic acid (0.25 mol) at 10–15 °C and reaction mixture was stirred for about 18 h. The reaction mixture then poured onto ice/water (200 ml). The product was extracted with ether. The ethereal solution was washed with water, dried over sodium sulfate and evaporated to give 4-(2-(4-chlorophenyl)-2-oxoethyl)benzene-1-sulfonyl chloride (**4b**). To a stirred solution of sodium sulfite (12.6 mmol) and sodium hydrogen carbonate (13.56 mmol) in water (25 ml) was added the compound **4b** (9.03 mmol) in tetrahydrofuran (10 ml). The reaction mixture was heated at 75 °C for 2 h and cooled to 30 °C and methyl iodide (45.2 mmol) was added. After being stirred at 50 °C for 24 h, the reaction mixture was cooled to room temperature and partitioned between water (50 ml) and ethyl acetate (100 ml). The aqueous

Table 5
In vivo anti-inflammatory activity of compounds.

Treatment[a]	Mean paw volume (ml) ± SEM[b]					% Inhibition of edema				
	1 h	2 h	3 h	4 h	24 h	1 h	2 h	3 h	4 h	24 h
Control	2.22 ± 0.071	2.10 ± 0.111	1.97 ± 0.002	1.68 ± 0.101	1.54 ± 0.056	–	–	–	–	–
5a	1.67 ± 0.015	1.71 ± 0.071	1.24 ± 0.090	1.49 ± 0.021	1.48 ± 0.050	24.77	18.57	37.06	11.31	3.90
5b	1.66 ± 0.071	1.59 ± 0.075	1.57 ± 0.064	1.50 ± 0.071	1.65 ± 0.045	25.23	24.29	20.30	10.71	–
5c	1.18 ± 0.060	1.23 ± 0.062	1.44 ± 0.019	1.52 ± 0.021	1.59 ± 0.088	46.85	41.43	26.90	9.52	–
5d	1.43 ± 0.077	1.70 ± 0.046	1.49 ± 0.061	1.39 ± 0.086	1.77 ± 0.047	35.59	19.05	24.37	17.26	–
5e	1.74 ± 0.034	1.51 ± 0.013	1.20 ± 0.092	1.71 ± 0.038	1.88 ± 0.089	21.62	28.10	39.09	–	–
5f	1.18 ± 0.057	1.45 ± 0.071	1.12 ± 0.091	1.37 ± 0.098	1.81 ± 0.101	46.85	30.95	43.15	18.45	–
5g	1.88 ± 0.080	1.54 ± 0.085	1.77 ± 0.083	1.76 ± 0.036	1.79 ± 0.039	15.32	26.67	10.15	–	–
5h	1.55 ± 0.073	1.67 ± 0.015	1.11 ± 0.080	1.20 ± 0.093	1.30 ± 0.066	30.18	20.48	43.65	28.57	15.58
5i	1.82 ± 0.041	1.52 ± 0.060	1.40 ± 0.042	1.41 ± 0.034	1.66 ± 0.065	18.02	27.62	28.93	16.07	–
5j	1.82 ± 0.040	1.51 ± 0.061	1.49 ± 0.042	1.44 ± 0.030	1.69 ± 0.07	18.02	28.10	24.37	14.29	–
Celecoxib	1.15	1.22	1.33	1.38	1.44	48.20	41.90	32.49	17.86	6.49

[a] Compounds were administered at a dose of 20 mg kg^{-1}.
[b] $n = 6$.

layer was then separated and further extracted with ethyl acetate (2 × 80 ml). The combined extracts were then dried over anhydrous Sodium sulfate, and the solvent was evaporated under vacuum to give compound **4d**.

Yield (solid): 46.4%; M.P.: 157–159 °C; FT-IR (neat) cm^{-1}: 3012, 2958, 1678, 1284; ^{1}H NMR (400 MHz, $CDCl_3$): $\delta = 3.30$ (s, 3H), 4.32 (s, 2H), 7.12 (d, 2H), 7.38–7.41 (m, 4H), 7.93 (d, 2H); ^{13}C NMR (400 MHz, $CDCl_3$): $\delta = 41.57$, 43.30, 119.24, 124.14, 127.56, 131.10, 133.15, 189.24; AP-MS: $m/z = 309.1$ $[M + H]^+$.

4.2.3. Synthesis of 4-(2-(4-chlorophenyl)-2-oxoethyl) benzenesulfonamide (*4e*)

4-(2-(4-chlorophenyl)-2-oxoethyl)benzene-1-sulfonyl chloride (**4b**) (0.0525 mol) was grinded with ammonium carbonate in a mortar until a fine uniform powder was obtained. The mixture was heated in an evaporating dish on water bath for 1–2 h and stired frequently with glass rod. The mixture was then Allowed to cool and extracted with little cold water to remove the excess of ammonium salts. The product obtained was then recrystallized from ethanol.

Yield (solid): 73.6%; M.P.: 192–194 °C; FT-IR (neat) cm^{-1}: 3410, 3385, 3010, 2951, 1682, 1280; ^{1}H NMR (400 MHz, $CDCl_3$): $\delta = 2.44$ (s, 2H), 4.40 (s, 2H), 7.22–7.36 (m, 6H), 7.88 (d, 2H); ^{13}C NMR (400 MHz, $CDCl_3$): $\delta = 42.12$, 119.30, 122.43, 128.35, 130.40, 134.50, 191.20; AP-MS: $m/z = 310.2$ $[M + H]^+$.

4.2.4. General procedure for synthesis of final compounds (*5a–j*)

A mixture of compound **4a**/**4d**/**4e** (0.06 mol), urea/thiourea/guanidine hydrochloride (0.06 mol), aldehyde (0.06 mol) and K_2CO_3 (0.06 mol) in 100 ml ethanol was refluxed in oil bath for 8–12 h. The completion of reaction was monitored on TLC. The reaction mixture was then poured onto ice–water mixture and the solid obtained was filtered. The product obtained was filtered, dried and recrystallized from ethanol.

Table 6
In vitro COX-2 and COX-1 enzymes inhibition data.

Sr. no.	Compound	COX-2 inhibition (%)[a]	COX-1 inhibition (%)
1	**5c**	46.23 ± 0.38	2.36
2	**5g**	39.45 ± 0.15	1.67
3	Celecoxib	49.23 ± 0.23	NI[b]

[a] Data are indicated as percentage of inhibition at 20 μM ± SEM.
[b] No inhibition obtained.

4.2.4.1. 4-(3,4-Dimethoxyphenyl)-6-(4-(methylsulfonyl)phenyl)-5-phenyl-3,4 dihydropyrimidin-2(1H)-imine (*5a*).

Yield (solid): 69%; M.P.: 97.2–99.7 °C; FT-IR (neat) cm^{-1}: 3344, 3029, 2923, 1260, 1220, 1150; ^{1}H NMR (400 MHz, $CDCl_3$): $\delta = 2.95$ (s, 3H), 3.64 (s, 3H), 3.80 (s, 3H), 5.14 (s, 1H), 6.67–7.05 (m, 5H), 7.26–7.44 (m, 7H), 7.65–7.67 (d, 2H), 9.85 (s, 1H); ^{13}C NMR (400 MHz, $CDCl_3$): $\delta = 44.42$, 55.86, 76.71, 119.16, 128.35, 130.40; AP-MS: $m/z = 464.5$ $[M + H]^+$; Elemental Anal. Calcd for $C_{25}H_{25}N_3O_4S$ (463.55), requires (Found): C 64.78 (64.77); H, 5.44 (5.41); N 9.06 (9.04).

4.2.4.2. 4-(2,5-Dimethoxyphenyl)-6-(4-(methylsulfonyl)phenyl)-5-phenyl-3,4-dihydropyrimidin-2(1H)-imine (*5b*).

Yield (Solid): 69.91%; M.P.: 81.4–83.6 °C; FT-IR (neat) cm^{-1}: 3360, 3015, 2880, 1258, 1210, 1134; ^{1}H NMR (400 MHz, $CDCl_3$): $\delta = 2.97$ (s, 3H), 3.71 (s, 3H), 3.77 (s, 3H), 5.60 (s, 1H), 6.76–6.91 (m, 5H), 7.03–7.26 (m, 5H), 7.53–7.55 (d, 2H), 7.71–7.73 (d, 2H), 10.44 (s, 1H); ^{13}C NMR (400 MHz, $CDCl_3$): $\delta = 44.49$, 55.63, 76.72, 114.88, 128.13, 130.57, 153.92; AP-MS: $m/z = 464.5$ $[M + H]^+$; Elemental Anal. Calcd for $C_{25}H_{25}N_3O_4S$ (463.55), requires (Found): C, 64.78 (64.75); H, 5.44 (5.43); N, 9.06 (9.03).

4.2.4.3. 4-(4-(Dimethylamino)phenyl)-6-(4-(methylsulfonyl)phenyl)-5-phenyl-3,4-dihydropyrimidin-2(1H)-one (*5c*).

Yield (solid): 51.4%; M.P.: 80.1–82.9 °C; FT-IR (neat) cm^{-1}: 3295, 3034, 2912, 1642, 1275, 1145; ^{1}H NMR (400 MHz, $CDCl_3$): $\delta = 3.29$ (s, 6H), 3.36 (s, 3H), 5.77 (s, 1H), 7.27–7.33 (m, 8H), 8.02–8.10 (m, 5H), 8.26–8.28 (d, 2H); ^{13}C NMR (400 MHz, $CDCl_3$): $\delta = 39.06$, 56.28, 126.64, 129.22, 140.31; AP-MS: $m/z = 448.2$ $[M + H]^+$. Elemental Anal. Calcd for $C_{25}H_{25}N_3O_3S$ (447.55); requires (Found): C, 67.09 (67.06); H, 5.63 (5.61); N, 9.39 (9.9.37).

4.2.4.4. 4-(2,5-Dimethoxyphenyl)-6-(4-(methylsulfonyl)phenyl)-5-phenyl-3,4-dihydropyrimidin-2(1H)-one (*5d*).

Yield (solid): 52%; M.P.: 62.5–64.0 °C; FT-IR (neat) cm^{-1}: 3348, 3095, 2984, 1632, 1212, 1140; ^{1}H NMR (400 MHz, $CDCl_3$): $\delta = 3.05$ (s, 3H), 3.68 (s, 3H), 3.72 (s, 3H), 5.15 (s, 1H) 6.68–6.80 (m, 3H), 6.84–6.96 (m, 3H), 7.02–7.28 (m, 6H), 9.02 (s, 2H); ^{13}C NMR (400 MHz, $CDCl_3$): $\delta = 45.12$, 56.72, 77.18, 115.52, 128.24, 130.15, 140.78; AP-MS: $m/z = 465.4$ $[M + H]^+$. Elemental Anal. Calcd for $C_{25}H_{24}N_2O_5S$ (464.53); requires (Found): C, 64.64 (64.61); H, 5.21 (5.19); N, 6.03 (6.00).

4.2.4.5. 4-(2,4-Dimethoxyphenyl)-6-(4-(methylsulfonyl)phenyl)-5-phenyl-3,4-dihydropyrimidin-2(1H)-one (*5e*).

Yield (solid): 51.6%; M.P.: 84.3–84.1 °C; FT-IR (neat) cm^{-1}: 3405, 3078, 2905, 1640, 1224, 1120; ^{1}H NMR (400 MHz, $CDCl_3$): $\delta = 2.51$ (s, 3H), 3.24 (s, 3H), 3.26

(s, 3H), 5.41 (s, 1H), 6.80–7.31 (m, 8H), 7.35–7.78 (m, 4H), 10.12 (s, 2H); ^{13}C NMR (400 MHz, $CDCl_3$): δ = 43.12, 55.38, 76.21, 126.54, 130.40, 144.31; AP-MS: m/z = 465.4 $[M + H]^+$. Elemental Anal. Calcd for $C_{25}H_{24}N_2O_5S$ (464.53); requires (Found): C, 64.64 (64.63); H, 5.21 (5.20); N, 6.03 (6.01).

*4.2.4.6. 6-(4-(Methylsulfonyl)phenyl)-4,5-diphenyl-3,4-dihydropyrimidine-2(1H)-thione (**5f**).* Yield (solid): 55.2%; M.P.: 117.6–118.8 °C; FT-IR (neat) cm^{-1}: 3356, 3055, 2925, 1144, 1085; ^{1}H NMR (400 MHz, $CDCl_3$): δ = 2.68 (s, 3H), 5.28 (s, 1H), 6.77–6.78 (d, 2H), 7.04–7.32 (m, 8H), 7.34–7.49 (m, 4H), 7.79–7.87 (d, 2H); ^{13}C NMR (400 MHz, $CDCl_3$): δ = 43.77, 61.32, 115.16, 127.84, 129.54, 141.00; AP-MS: m/z = 421.3 $[M + H]^+$. Elemental Anal. Calcd for $C_{23}H_{20}N_2O_2S_2$ (420.55); requires (Found): C, 65.69 (65.53); H, 4.79 (4.65); N, 6.66 (6.54).

*4.2.4.7. 4-(2,4-Dimethoxyphenyl)-6-(4-(methylsulfonyl)phenyl)-5-phenyl-3,4-dihydropyrimidine-2(1H)-thione (**5g**).* Yield (solid): 54.2%; M.P.: 84.0–86.1 °C; FT-IR (neat) cm^{-1}: 3345, 3025, 2943, 1223, 1134, 1074; ^{1}H NMR (400 MHz, $CDCl_3$): δ = 2.68 (s, 3H), 3.87 (s, 3H), 3.90 (s, 3H), 5.86 (s, 1H), 7.17–7.49 (m, 6H), 7.51–7.80 (m, 6H), 10.28 (s, 2H); ^{13}C NMR (400 MHz, $CDCl_3$): δ = 44.40, 55.48, 77.04, 124.10, 128.86, 140.82; AP-MS: m/z = 481.2 $[M + H]^+$. Elemental Anal. Calcd for $C_{25}H_{24}N_2O_4S_2$ (480.60); requires (Found): C, 62.48 (62.33); H, 5.03 (4.95); N, 5.83 (5.74).

*4.2.4.8. 6-(4-Chlorophenyl)-4-(4-methoxyphenyl)-5-(4-(methylsulfonyl)phenyl)-3,4-dihydropyrimidin-2(1H)-imine (**5h**).* Yield (solid): 64.1%; M.P.: 122.0–124.1 °C; FT-IR (neat) cm^{-1}: 3395, 3043, 2958, 1215, 1130; ^{1}H NMR (400 MHz, $CDCl_3$): δ = 3.29 (s, 3H), 3.67 (s, 3H), 5.51 (s, 1H), 7.24–7.31 (m, 7H), 7.42–7.49 (m, 5H), 8.75–8.78 (d, 2H), 10.31 (s, 1H); ^{13}C NMR (400 MHz, $CDCl_3$): 39.21, 55.84, 76.91, 112.80, 124.99, 134.55, 153.21; AP-MS: m/z = 468.3 $[M + H]^+$. Elemental Anal. Calcd for $C_{24}H_{22}ClN_3O_3S$ (467.11); requires (Found): C, 61.60 (61.56); H, 4.74 (4.65); N, 8.98 (8.84).

*4.2.4.9. 6-(4-Chlorophenyl)-4-(4-(dimethylamino)phenyl)-5-(4-(methylsulfonyl)phenyl)-3,4-dihydropyrimidin-2(1H)-one (**5i**).* Yield (solid): 61.2%; M.P.: 108.2–110.0 °C; FT-IR (neat) cm^{-1}: 3380, 3058, 2930, 1635, 1256, 1138; ^{1}H NMR (400 MHz, $CDCl_3$): δ = 2.79 (s, 6H), 3.09 (s, 3H), 5.39 (s, 1H), 7.02–7.18 (m, 4H), 7.22–7.42 (m, 4H), 7.90–7.96 (m, 4H), 9.78 (s, 2H); ^{13}C NMR (400 MHz, $CDCl_3$): 40.12, 56.82, 123.12, 132.56, 141.10; AP-MS: m/z = 482.1 $[M + H]^+$. Elemental Anal. Calcd for $C_{25}H_{24}ClN_3O_3S$ (481.12); requires (Found): C, 62.30 (62.26); H, 5.02 (4.96); N, 8.72 (8.66).

*4.2.4.10. 4-(6-(4-Chlorophenyl)-4-(2,5-dimethoxyphenyl)-2-oxo-1,2,3,4-tetrahydropyrimidin-5-yl)benzenesulfonamide (**5j**).* Yield (solid): 51.2%; M.P.: 105.8–107.1 °C; FT-IR (neat) cm^{-1}: 3375, 3284, 3032, 2956, 1638, 1219, 1129; ^{1}H NMR (400 MHz, $CDCl_3$): δ = 2.98 (s, 2H), 3.82 (s, 3H), 3.94 (s, 3H), 5.42 (s, 1H), 6.82–7.04 (m, 6H), 7.08–7.22 (m, 5H), 9.06 (s, 2H); ^{13}C NMR (400 MHz, $CDCl_3$): 41.20, 57.12, 78.12, 113.14, 125.86, 134.12, 140.02; AP-MS: m/z = 500.6 $[M + H]^+$. Elemental Anal. Calcd for $C_{24}H_{22}ClN_3O_5S$ (499.97); requires (Found): C, 57.66 (57.44); H, 4.44 (4.26); N, 8.40 (8.36).

4.3. Pharmacological studies

4.3.1. In vivo anti-inflammatory activity

Albino rats of either sex (150–200 g) were divided into different groups, containing six animals each. Animals were fasted for 12 h before experiment and only water was allowed. The first group was a control and received vehicle (Tween 80 in propylene glycol (10%, v/v), 0.5 ml per rat), the second group received celecoxib 20 mg kg^{-1} body mass. All the remaining groups received the test compounds at the same dose orally. All the suspensions for oral dose were prepared in the vehicle mentioned above and administered in a constant volume of 0.5 ml per rat. After 1 h of the administration of the test compound and celecoxib, 0.1 ml of 1% w/v suspension of carrageenan was injected in to the subplanatar of left paw of control and test animals. Immediately, the paw volume was measured using Plethysmometer (initial paw volume), there after the paw volume was measured every 1 h till 4 h. The difference between initial and subsequent readings gave the edema volume for the corresponding time. Percentage inhibition was calculated.

4.3.2. In vitro cyclooxygenase (COX) inhibition assays

The assay was performed using colorimetric COX (ovine) inhibitor screening assay kit (Cayman chemical, MI, USA). The assay utilizes the peroxidase activity of ovine cyclooxygenase to oxidize the colorimetric substrate, *N*,*N*,*N*′,*N*′-tetramethyl-*p*-phenylenediamine (TMPD). Enzyme assays were performed with total volume of 220 μl. The mixture in background wells, 100% initial activity wells and inhibitor wells were prepared according to the instructions provided by the manufacturers and preincubated for 5 min at 25 °C. The reaction was initiated by addition of 20 μl of TMPD solution followed by 20 μl of arachidonic acid in all the wells. The assay mixture was mixed thoroughly and incubated at 25 °C for 5 min. The enzyme activity was determined by measuring absorbance at 590 nm in a microplate reader.

Acknowledgments

The authors are thankful to University Grant Commission (UGC), New Delhi for financial assistance. The authors are also thankful to the Head, Department of Chemical Technology, Dr. Babasaheb Ambedkar Marathwada University, Aurangabad 431 004 (MS), India for providing the laboratory facility.

Appendix A. Supplementary data

Supplementary data related to this article can be found at http://dx.doi.org/10.1016/j.ejmech.2013.10.083.

References

[1] K. Seibert, Y. Zhang, K. Leahy, S. Hauser, J. Masferrer, W. Perkins, L. Lee, P. Isakson, Pharmacological and biochemical demonstration of the role of cyclooxygenase 2 in inflammation and pain, Proc. Natl. Acad. Sci. U. S. A. 91 (1994) 12013–12017.
[2] T. Tanabe, N. Tohnai, Cyclooxygenase isozymes and their gene structures and expression, Prostaglandins Other Lipid Mediat. 68–69 (2002) 95–114.
[3] C. Sakamoto, S. Soen, Efficacy and safety of the selective cyclooxygenase-2 inhibitor celecoxib in the treatment of rheumatoid arthritis and osteoarthritis in Japan, Digestion 83 (2011) 108–123.
[4] A. Lanas, A review of the gastrointestinal safety data – a gastroenterologist's perspective, Rheumatology 49 (2010) ii3–ii10.
[5] W.L. Smith, I. Song, The enzymology of prostaglandin endoperoxide H synthases-1 and -2, Prostaglandins Other Lipid Mediat. 68–69 (2002) 115–128.
[6] R.M. Garavito, M.G. Malkowski, D.L. DeWitt, The structures of prostaglandin endoperoxide H synthases-1 and -2, Prostaglandins Other Lipid Mediat. 68–69 (2002) 129–152.
[7] O. Unsal-Tan, K. Ozadali, K. Piskin, A. Balkan, Molecular modeling, synthesis and screening of some new 4-thiazolidinone derivatives with promising selective COX-2 inhibitory activity, Eur. J. Med. Chem. 57 (2012) 59–64.
[8] R. Ghodsi, A. Zarghi, B. Daraei, M. Hedayati, Design, synthesis and biological evaluation of new 2,3-diarylquinoline derivatives as selective cyclooxygenase-2 inhibitors, Bioorg. Med. Chem. 8 (2010) 1029–1033.
[9] P.J. Beswick, A.P. Blackaby, C. Bountra, T. Brown, K. Browning, I.B. Campbell, J. Corfield, R.J. Gleave, S.B. Guntrip, R.M. Hall, S. Hindley, P.F. Lambeth, F. Lucas, N. Mathews, A. Naylor, H. Player, H.S. Price, P.J. Sidebottom, N.L. Taylor, G. Webb, J. Wiseman, Identification and optimisation of a novel series of pyrimidine based cyclooxygenase-2 (COX-2) inhibitors. Utilisation of a biotransformation approach, Bioorg. Med. Chem. Lett. 19 (2009) 4509–4514.

[10] D. Lokwani, R. Shah, S. Mokale, P. Shastry, D. Shinde, Development of energetic pharmacophore for the designing of 1,2,3,4-tetrahydropyrimidine derivatives as selective cyclooxygenase-2 inhibitors, J. Comput. Aided Mol. Des. 26 (2012) 267–277.
[11] S.S. Bahekar, D.B. Shinde, Synthesis and anti-inflammatory activity of some [4,6-(4-substituted aryl)-2-thioxo-1,2,3,4-tetrahydropyrimidin-5-yl]-acetic acid derivatives, Bioorg. Med. Chem. Lett. 14 (2004) 1733–1736.
[12] S.S. Bahekar, D.B. Shinde, Synthesis and anti-inflammatory activity of some (2-amino-6-(4-substituted aryl)-4-(4-substitutedphenyl)-1,6-dihydropyrimidine-5-yl)-acetic acid derivatives, Acta Pharm. 53 (2003) 223–229.
[13] M.E. Swarbrick, P.J. Beswick, R.J. Gleave, R.H. Green, S. Bingham, C. Bountra, M.C. Carter, L.J. Chambers, I.P. Chessell, N.M. Clayton, S.D. Collins, J.A. Corfield, C. David Hartley, S. Kleanthous, P.F. Lambeth, F.S. Lucas, N. Mathews, A. Naylor, L.W. Page, J.J. Payne, N.A. Pegg, H.S. Price, J. Skidmore, A.J. Stevens, R. Stocker, S.C. Stratton, A.J. Stuart, J.O. Wiseman, Identification of [4-[4-(methylsulfonyl)phenyl]-6-(trifluoromethyl)-2-pyrimidinyl] amines and ethers as potent and selective cyclooxygenase-2 inhibitors, Bioorg. Med. Chem. Lett. 19 (2009) 4504–4508.
[14] A. Nayyar, S.R. Patel, M. Shaikh, E. Coutinho, R. Jain, Synthesis, antituberculosis activity and 3D-QSAR study of amino acid conjugates of 4-(adamantan-1-yl) group containing quinolines, Eur. J. Med. Chem. 44 (2009) 2017–2029.
[15] A. Manvar, A. Malde, J. Verma, V. Virsodia, A. Mishra, Synthesis, antitubercular activity and 3D-QSAR study of coumarin-4-acetic acid benzylidene hydrazides, Eur. J. Med. Chem. 43 (2008) 2395–2403.
[16] V. Rao Veeramaneni, M. Pal, K. Rao Yeleswarapu, A high speed parallel synthesis of 1,2-diaryl-1-ethanones via a clean-chemistry C–C bond formation reaction, Tetrahedron 59 (2003) 3283–3290.